Spectroscopic and microscopic characterization of dipicolinic acid and its salt photoproducts – A UVc effect study on DPA in solution and in bacterial spores

Maxime Pacheco, Jonathan Dikec, Pascale Winckler, Jean-Marie Perrier-Cornet, Christian Coelho

Spectroscopic and microscopic characterization of dipicolinic acid and its salt photoproducts - A UVc effect study on DPA in solution and in bacterial spores.

Maxime Pacheco[1], Jonathan Dikec[1], Pascale Winckler[1,2], Christian Coelho[3], Jean-Marie Perrier-Cornet[1,2,*].

[1] *UMR Procédés Alimentaires et Microbiologiques, L'Institut Agro Dijon, Université de Bourgogne Franche-Comté, 1, Esplanade Erasme, 21000 Dijon, France.*

[2] *Dimacell Imaging Facility, L'Institut Agro Dijon, Université de Bourgogne Franche-Comté, 1 Esplanade Erasme, 21000 Dijon, France.*

[3]*Université Clermont Auvergne, INRAE, VetAgro Sup campus agronomique de Lempdes, UMR F, 15000 Aurillac, France.*

* Corresponding author.

E-mail address: jperrier@u-bourgogne.fr (J.-M. Perrier-Cornet)

Abstract:

Bacterial spores can cause significant problems such as food poisoning (like neurotoxin or emetic toxin) or serious illnesses (like anthrax or botulism). This dormant form of bacteria, made of several layers of barriers which provide extreme resistance to many abiotic stresses (radiation, temperature, pressure, etc.), are difficult to investigate *in situ*. To better understand the biological and chemical mechanisms involved and specific to spores resistance, the acquisition of environmental parameters is necessary. For that purpose, our research has been focused on the detection and analysis of a unique spore component, dipicolinic acid (DPA), used as the main *in situ* metabolite for sporulating bacteria detection. In its native form, DPA is only weakly fluorescent but after Ultraviolet irradiation at the wavelength of 254 nm (UVc), DPA photoproducts (DPAp) exhibit a remarkable fluorescence signal. These photoproducts are rarely identified and part of this study gives new insights offered by mass spectrometry (MS) in the determination of DPA photoproducts. Thanks to DPA assay techniques and fluorescence spectrometry, we highlighted the instability of photoproducts and introduced new assumptions on the effects of UVc on DPA. Studies in spectroscopy and microscopy allowed us to better understand these native probes in bacterial spores and will allow the implementation of a new method for studying the physico-chemical parameters of spore resistance.

Keywords:

Bacterial spore – DPA – Photoproducts – Native probe – Fluorescence lifetime – Phasor plot – Two-photon microscopy

1. Introduction

Bacterial spores are a dormant form of bacteria structured in several layers: exosporium (absent from *B. subtilis*), coats, outer membrane, cortex, inner membrane and a core; which result in high resistance to extreme conditions [1,2]. These structures are mainly composed of lipids, polysaccharides or proteins. Because of its multilayer structure, the molecules and their structure involved in the resistance properties of this bacterial form are difficult to study separately. Moreover, analysis often requires invasive or destructive methods. There is a need to determine the physico-chemical parameters of bacterial spores leading to their resistance. These parameters should be measured inside the spore core. The investigation difficulties explain the lack of knowledge concerning the physical state and mobility of spore core. The form of CaDPA inside the spore core is not clear, some authors suggest, for example, that CaDPA is probably present in a powder form inside the spore [3]. Moreover, pH inside the spore core and water activity are still not been easily measured *in vivo* and require destructive or complex methods to be investigated. These parameters are important for spore resistance against physical stresses used in sterilization processes like wet heat resistance or even UV resistance. Having new insights of what are the precise internal physico-chemical parameters could lead to the development of more precise and destructive methods to sterilize spores in food matrix and avoid spoilage or diseases caused by pathogenic sporulated bacteria. To achieve this objective, it is interesting to look at native probes (intrinsic probes in the medium) present in bacterial spores. There are two native biomolecules sufficiently concentrated in the core that could govern spore resistance, particularly against temperature and UV exposure. Water is the first of these molecules as H_2O makes up 27-55% of the spore core wet weight depending on the species [4–6]. Dipicolinic acid, also named 2,6-pyridinedicarboxylic acid (DPA) is the second core molecule involved in spore resistance [7–9]. DPA is involved in low water activity of the spore core. This gives the bacterial spore its high thermal resistance properties. DPA is a specific spore molecule present in large quantities in bacterial spores (5-15% of spore dry weight) [10]. DPA is located only in the core, and Raman spectroscopy showed that it should be present in equimolar amounts with calcium, as CaDPA [3]. The use of DPA and CaDPA as a probe for the study of bacterial spores has been largely documented [11–16]. Those studies used destructive methods of the spore structures to extract DPA outside the core. Another approach consists in analyzing the photoproduct forms of DPA and CaDPA (DPAp and CaDPAp), because of their fluorescent emission properties

[17,18]. DPA and CaDPA are only very weakly fluorescent thus irradiation at 254 nm is required to create DPAp and CaDPAp that will emit fluorescence signals. This method has already been used for the analysis of bacterial spores [19,20] but very few publications succeeded in determining the characteristics of these photoproducts [21,22]. Even if DPA seems present mainly in chelated forms, particularly with calcium, studies showed the interest in studying both compounds (DPA and CaDPA) because of the sensitivity of fluorescence to diagnose environmental conditions of bacterial spores [18].

This paper aims to discuss the photochemical effect of UVc on DPA and CaDPA and to characterize the resulting molecules DPAp and CaDPAp to detect them in bacterial spores. For that purpose, the fluorescence of these photoproducts was investigated with excitation emission matrices of fluorescence (EEMF) and emission spectra at fixed excitation wavelengths. The characterization of photoproducts and their stability has been studied using various techniques, such as the dosage of Terbium-DPA complex and mass spectrometry. The visualization of its photoproducts was carried out by multi-photon microscopy techniques and by analysis of the fluorescence lifetimes associated with these molecules.

2. Materials and Methods

2.1. Chemicals

DPA (Sigma-Aldrich, Germany, 167.12 g/mol, purity > 98 %) solution (10 mM) was prepared in water and stored at room temperature. The pH was adjusted to 8 with a Tris base buffer (Sigma-Aldrich, Germany, 121 g/mol, purity > 99.9 %). CaDPA solution (50 mM) was prepared with a 1:1 mix of DPA solution and $CaCl_2$ (Sigma-Aldrich, Germany, 110.98 g/mol, purity > 96 %).

2.2. Bacterial strains and culture conditions

B. subtilis strains used in this study were PS533 (wild-type), PS4150 and FB122. PS533 was obtained from the courtesy of P. Setlow from the Department of Molecular, Microbial, and Structural Biology, University of Connecticut Health Center, USA. This strain was carrying a plasmid encoding resistance to kanamycin. PS4150 was a strain that was unable to form the majority of proteins from the outer coat layer because of the deletion of cotE and gerE coding sequences, making this strain non autofluorescent [23]. FB122 was a strain deleted for the spoVF operon and SleB gene, resulting in a strong depletion of DPA content [7].

For spores production, the different strains were first isolated on LB agar medium containing antibiotics (10µg/mL of kanamycin for PS533, spectinomycin 100 µg/ml + 10µg/mL tetracycline for PS4150 and FB122) at 37°C for 12h. An isolated colony was then placed on double strength Schaeffer's-glucose liquid medium (2xSG) at 37°C under agitation until reaching an OD of 0.6. Then the culture was diluted 10 times on a fresh 2xSG medium and incubated under agitation 5 days at 37°C. All purified spores were washed at least 3 times with sterilized distilled water at 4°C until 98% purity was reached and stored at 4°C.

2.3. Photolysis conditions

Ultraviolet (UV) corresponds to wavelengths of light between about 100 and 400 nm, that are divided into several categories according to their ranges in this spectrum (UVa, UVb and UVc). The wavelength used for the photolysis is 254 nm, which correspond to UVc. UVc irradiation of DPA and CaDPA solutions was performed in distilled water, by means of a UV irradiation system CROSSLINKER® CL-508 (UVItec Ltd, UK) with 5 UVc tubes at 0.120 J/cm². For the mass spectrometry (MS) experiment, DPA with greater purity (Sigma-Aldrich, Germany, 167.12 g/mol, purity > 99.5 %) (3 g/L) was diluted in ultrapure water. Water was removed after irradiation using a rotary evaporator. The residues of DPAp for each irradiation time were dissolved in methanol solution (Sigma-Aldrich, Germany, Chromasolv™ for HPLC min. 99.9 %). Irradiations of bacterial spores were performed in a liquid sample by means of 2 minutes UVc irradiation at 0.120 J/cm², at a concentration of 1.10^7 cell/ml to avoid any shielding effect [24].

2.4. Steady state fluorescence

Excitation-emission matrices of fluorescence (EEMF) was acquired on a Horiba Aqualog (Horiba Scientific, Kyoto, Japan) unit by setting the excitation wavelengths from 225 nm to 600 nm (3 nm interval) and the emission wavelengths from 200 to 600 nm (3.22 nm). Each EEMF was corrected daily for Rayleigh scattering and inner filtering. It was normalized to a 1ppm quinine sulphate solution using the manufacturer's software (Aqualog software).

Emission spectra were acquired on a Jobin Yvon Fluorolog 3 (Horiba Scientific, Kyoto, Japan) by setting the excitation wavelengths at 300 nm and 340 nm and the emission wavelengths from 380 to 500 nm with a 5 nm bandpass and a 1 nm step.

2.5. DPA assay

DPA assay was performed according to the protocol proposed by Hindle and Hall (1999). This stock solution of 0.1 mM DPA was prepared in a 16 g/L NaOH solution (Sigma-Aldrich, Germany, 40.00 g/mol, purity > 98 %). Different volumes of this DPA were added to 3 mL of 1 M acetate buffer

($C_2H_3NaO_2.3H_2O$, Sigma-Aldrich, Germany, 136.08 g/mol, purity > 99 %) (pH 5.6) and 3 µL of 10 mM $TbCl_3$ solution (Sigma-Aldrich, Germany, 373.38 g/mol, purity = 99.9 %) in quartz cuvettes to make the standard curve. Emission spectra were acquired on a Jobin Yvon FluoroMax-4 (Horiba Scientific, Kyoto, Japan). The excitation and emission wavelengths were 280 ± 10 nm and 545 ± 5 nm respectively. A glass slide was placed in front of the detector to filter the Rayleigh diffusion of water. The standard curve can be found in Supplementary Information (S.I.) Fig. S1 & S2.

2.6. Q-ToF MS analysis

Direct injection of DPA solution (3g/L in methanol) and DPAp identification was performed with a MaXis plus MQ ESI-Q-TOF mass spectrometer (Bruker, Bremen, Germany). MS experiments aim of identifying new photoproducts, and was not a quantitative method. Acquisitions were done in the *m/z* 100 to 1500 mass range in positive ionization mode with an electrospray ionization source. The injection flow was 200 µL/h, the nebulization pressure was 2 bar and the dry nitrogen flow was 10 L/min. The mass spectrometer parameters were 500 V for end plate offset and 4500 V for capillary voltage. Before analysis, the mass spectrometer was calibrated by injecting Na Formate clusters. This calibration was realized in “enhanced quadratic” mode with an error of less than 0.5 ppm. Data were treated using Compass DataAnalysis v4.3 software (Bruker, Bremen, Germany). Elementary formula were determined using an isotopic profile.

2.7. Multi-photon & fluorescence lifetime microscopy

Fluorescence lifetime images were collected using a time-correlated single-photon counting (TCSPC) module (Picoquant, Germany) on a Nikon A1-MP scanning microscope equipped with a Plan Apo IR x 60 objective (NA: 1.27, Water Immersion, Nikon, Japan) at a scanning speed of 1 frame per second. A 700 nm excitation was provided by an IR laser (Chameleon, Coherent, California) delivering femtosecond pulses at a repetition rate of 80 MHz. Fluorescence emission of spores was collected on three detection channels for multiphoton imaging: FF01-492/SP-25 (400-492 nm), FF03-525/50-25 (500-550 nm) and FF01-575/25-25 (563-588 nm) (Semrock, USA). For fluorescence lifetime imaging, fluorescence was collected through a band-pass emission filter 680/SP (Semrock, USA). TCSPC recording was performed over 200 temporal channels (final resolution 0.64 ps). We performed fluorescence lifetime image acquisition on spores using Symphotime software (Picoquant, Germany). Then fluorescence lifetimes were calculated by using the MAPI software (See next paragraph).

2.8. Time resolved fluorescence analysis

Fluorescence lifetime is a photo-physical parameter that varies with the conformation of the fluorophore molecule and with the external physico-chemical conditions of the local environment.

Fluorescence lifetime analysis was performed using the phasor plot representation provided by the MAPI software (IRI, USR 3078 CNRS, BCF, available on request at: http://biophotonique.univ-lille1.fr/spip.php?rubrique60) [26].

2.8.1. Phasor plot representation

The phasor plot is a graphical representation of the raw TCSPC data in a vector space obtained by the mathematical Fourier transform decomposition. Each fluorescence decay curve is converted into $[g\ ;\ s]$ coordinates, calculated by the cosine and sine transforms of the measured fluorescence intensity decay I(t), defined by:

$$g(\omega) = \frac{\int_0^T I(t)\,.\cos(n\omega t)dt}{\int_0^T I(t)\,d(t)} \qquad (3)$$

$$s(\omega) = \frac{\int_0^T I(t)\,.\ \sin(n\omega t)dt}{\int_0^T I(t)\,d(t)} \qquad (4)$$

Where ω is the laser repetition angular frequency, n is is the harmonic frequency and T is the finite width of the temporal measurement window. For a mono-exponential decay, the $[g\ ;\ s]$ coordinates are located on a semicircle centered on point [0.5;0] with a radius of s 0.5. Whereas for a multi-exponential decay, the $[g\ ;\ s]$ coordinates will no longer be located on the semicircle but rather inside this semicircle. In the semicircle, the short fluorescence lifetimes are close to the coordinates [1;0], and the long fluorescence lifetimes approach the origin [0;0].

2.9. Statistical analysis

The DPA concentration and fluorescence intensity of bacterial spores were statistically analyzed with a variance analysis (ANOVA performed with Origin® (OriginLab®, USA), p-value <0.05) to evaluate the differentiation significance between before and after UVc irradiation.

3. Results & Discussion

3.1. Stationary spectroscopy on DPAp and CaDPAp

Fig. 1 shows the effect of UVc irradiation on DPA (10 mM) and CaDPA (50 mM). Untreated DPA and CaDPA were very weakly fluorescent, which was already known [17]. After the UVc treatment, there were no changes in wavelengths of maximum absorbance (to collect the absorbance spectra, the solutions were diluted which did not change the couples excitation/emission wavelengths (EX/EM) (S.I. Fig. S3 & S4)). The EEMFs of DPAp and CaDPAp solution highlight the presence of two groups of fluorophores at EX/EM (nm): 340/430 nm and another one at 300/400 nm. The first group of

fluorophores with the EX/EM couple of 340/430 nm were mainly present in the DPAp solution but also observed in the CaDPAp solution. However, in CaDPAp solution, it was the group of fluorophores at the couple EX/EM of 300/400 nm that had the most influence on the fluorescence intensity. These results were in accordance with the literature [17–19]. Those EEMF showed at the same time the influence of the calcium salt on the fluorescence of the photoproducts and the importance of working at two different EX/EM couples to target and distinguish DPAp/CaDPAp fluorophores.

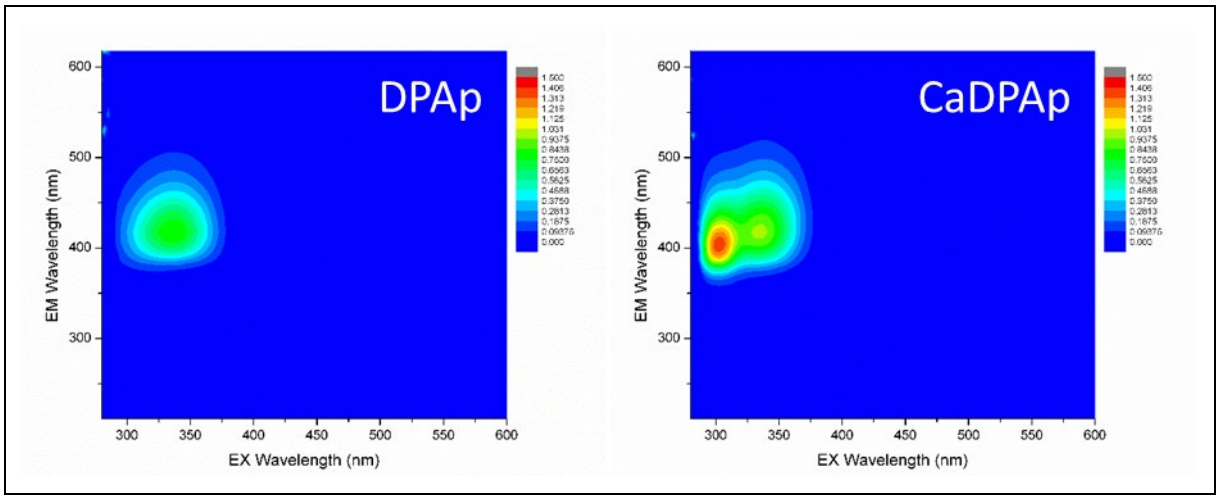

Figure 1: UVc irradiation (λ_{ex}: 254 nm, 10 min at 0.120 J/cm²) on DPA (10mM) and CaDPA (50mM). EEMF of resulting photoproducts: DPAp and CaDPAp. DPA and CaDPA EEMF were not shown because the compounds did not emit enough fluorescence to be detected. The same intensity (a.u.) scale was used for all spectra.

To confirm the previous results and observe the stability of the photoproducts, emission spectra were obtained for DPA and CaDPA before and after UVc treatment. As shown in Fig. 2, the fluorescence intensity significantly increased with irradiation (10 min at 0.120J/cm²). For DPA, the maximum of fluorescence intensity increased respectively by 156 and 216 times for EX/EM couples of 340/430 nm and 300/400 nm. For CaDPA, the maximum of fluorescence intensity increased respectively by 21 and 22 times. However, these experiments also highlighted that the photoproducts were partly unstable. For DPAp and CaDPAp, and for each EX/EM couple, the fluorescence intensity blatantly increased, by 1.6 to 3.4 times after 24 hours. A possible hypothesis of such instability of DPAp/CaDPAp obtained after UVc treatment could be attributed to the aromatic ring stretch and the bonds of the acidic functional groups becoming shortened [27]. These changes in the conformation of the molecule, and possibly others, may be responsible for the instability of DPAp. Subsequently the rearrangement of part of excited DPA or CaDPA (DPA* or CaDPA*) is probably oriented towards the production of photoproducts, which may explain the slight increase in fluorescence intensity.

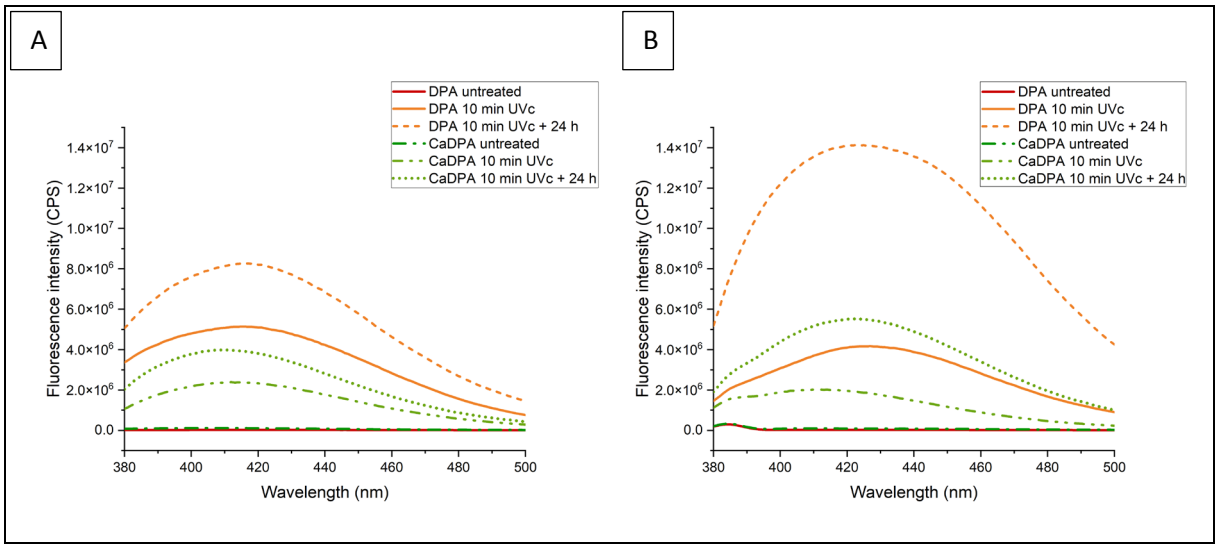

Figure 2: Fluorescence emission spectra of DPA (10 mM) and CaDPA (50 mM) for two excitation wavelengths: λ_{ex}= 300 nm (A) and λ_{ex}= 340 nm (B). The red (DPA) and the dark green (CaDPA) lines were obtained before UVc treatment (irradiation of 10 min. at 0.120 J/cm²). The orange and light green solid line correspond to DPAp and CaDPAp emission spectra after irradiation. The corresponding dotted lines come from the same samples after 24h.

3.2. UVc effect on DPA

Complexation between DPA and certain lanthanides makes it possible to drastically increase DPA fluorescence, with emission bands characteristic of these complexes, it allows a quantitative and specific detection of DPA. Terbium was the best lanthanide for the detection of DPA, as it provides a greater fluorescence compared to other lanthanides [25]. For the DPA assay, we used $TbCl_3$ as lanthanide able to form highly fluorescent complex with DPA. As shown in Fig. 3(A), after UVc irradiation of 10 minutes at 0.120 J/cm², the concentration of a DPA solution initially close to 100 nM decreased to a mean value of 43.2 nM. For the same group of samples, after 24 hours of waiting, the DPA dosage leads to a significant increase of the DPA concentration up to a mean value of 59.8 nM. The same behavior was observed with another set of samples submitted to 20 minutes irradiation, as shown in Fig. 3(B). In this case, the DPA concentration decreased up to a mean value of 16.8 nM after the 20 minutes irradiation and increased up to a mean value of 23.6 nM after 24 hours. This behavior was observed on the same set of samples irradiated twice 10 minutes (S.I. Fig. S5). This experiment highlights the fact that excited DPA* reverts to the DPA form some time after irradiation, which to our knowledge, has never been demonstrated until now. Our hypothesis was clarified as follows: after a UVc irradiation, the DPA* will partly be transformed in photoproducts but a part of this DPA* stays in an unstable form. This unstable form of DPA* will then break down into two parts, a first that will return to its initial form of DPA and another part that will rearrange itself to form DPAp. Only a small part of this DPA* was supposed to rearrange into the photoproducts form, would have

explained the slight increase in fluorescence intensity after 24 hours, as observed in part 3.1 (Fig. 2(A) and 2(B)).

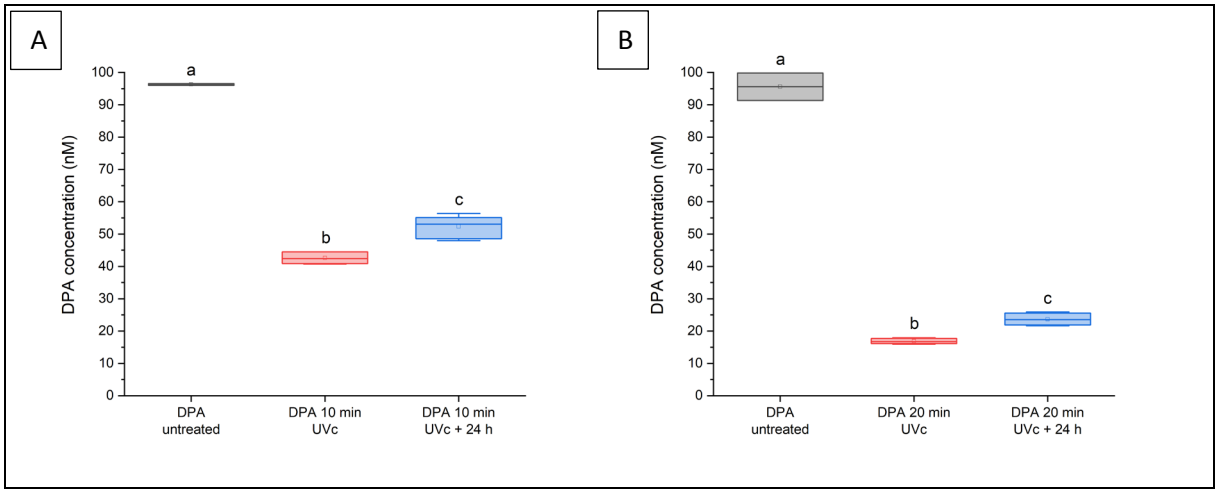

Figure 3: Analysis of variance of DPA concentration (nM) depending if DPA was dosed immediately after or 24 hours after the UVc irradiation. Two irradiation times were used: 10 min at 0.120 J/cm² (A) and 20 min at 0.120 J/cm² (B) with an initial DPA concentration of 100nM. Each irradiated group (N(A)=6; N(B)=4) was dosed directly after irradiation and 24 hours after irradiation. Different letters above box plot (a,b) represent significant differences (p=0.05) between the time conditions.

3.3. Identification of DPAp

The influence of the UVc treatment on the DPA was directly visible on our mass spectrometry spectra, shown in Fig. 4. There were five MS peaks significantly present before irradiation corresponding to *m/z* of 122.0236, 150.0184, 168.0290, 182.0447 and 190.0110. After irradiation of 10 min, many MS peaks appear at *m/z* of 12.0392, 130.1589, 157.0758, 186.2217, 201.0658, 202.2165, 217.0607, 245.0556, 261.0505, 270.5129 and 372.9975. We also observe the disappearance of a peak at 182.0447 that reappears for prolonged irradiation. By using longer irradiation time, the amount of certain photoproducts was amplified such as the molecules corresponding to the *m/z* at 124.0392, 157.0758, 201.0658 and 217.0607. This prolonged irradiation highlighted the consumption of one of the photoproduct present at the 202.2165 *m/z* peak.

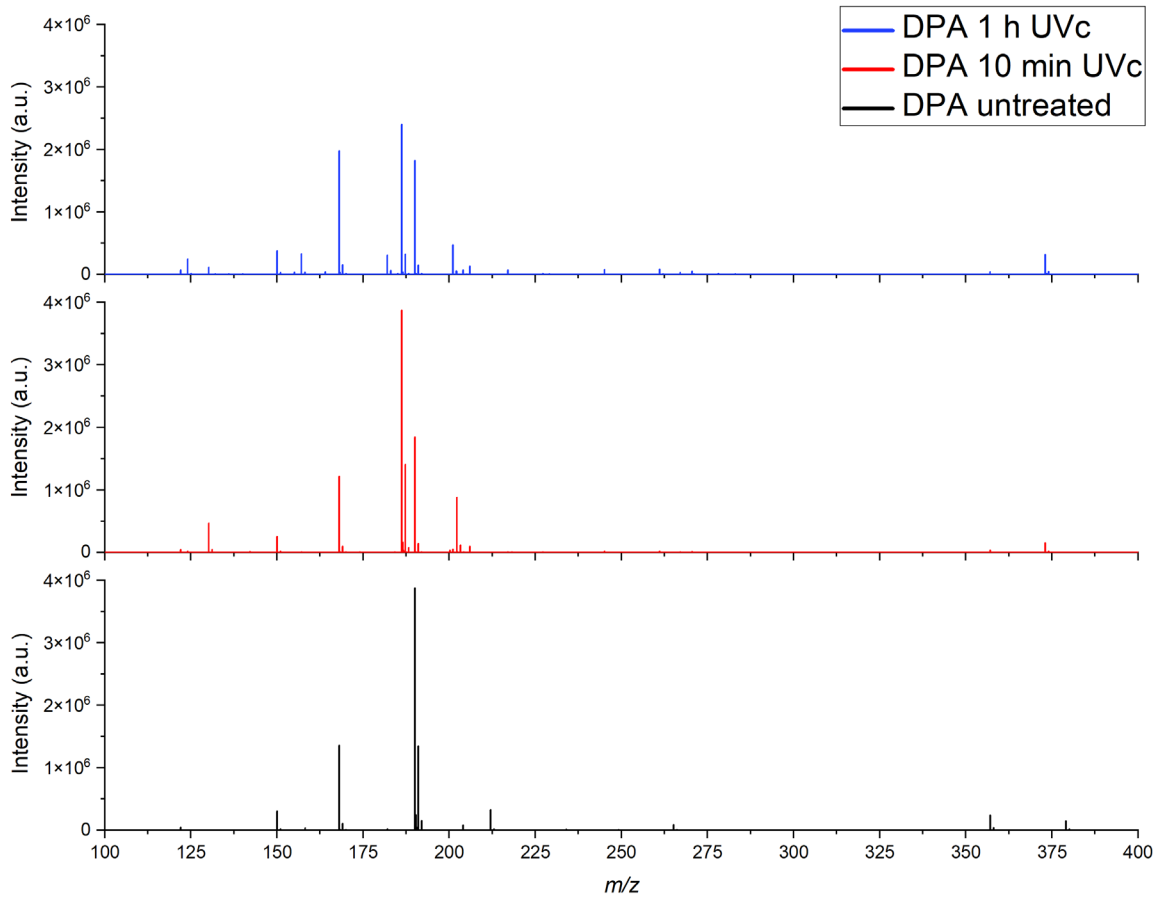

Figure 4: MS spectra obtained for DPA before and after UVc treatment (0.120 J/cm²) at different times (10 min and 1 h). Only m/z values from 100 to 400 were representing on the X-axis, as all changes occur in this range.

Based on the previous recent literature [21,22] and knowing the configuration of the DPA molecule, we were able to provide information concerning the identification of certain photoproducts and to propose structural formula, as shown in Table 1. These results were accompanied by a precision, Err in ppm, which represented the deviation from the theoretical monoisotopic mass, as well as an mSigma value, which represented the correspondence between theoretical and experimental isotopic profiles. The lower Err and mSigma values were, the stronger the correspondence was. The UVc treatment may allow the decarboxylation of one of the acidic functions of dipicolinic acid that would lead to the production of picolinic acid. This acid would serve as a precursor for the creation of bipyridine complexes such as Dimethyl 2,2'-Bipyridine-6,6'-dicarboxylate and Dimethyl 2,3'-Bipyridine-6,6'-dicarboxylate. The molar masses obtained in mass spectrometry were consistent with these compounds and support the proposed models.

The following putative compounds: $C_6H_4NO_2$, $C_7H_4NO_3$, $C_7H_6NO_4$, $C_8H_8NO_4$ and $C_4H_4N_3O_6$ were present in the DPA solution before UVc, which means that all these compounds were already present in

either DPA or the results of chemical reactions due to the solvent which was methanol. Among this list of compounds, some of them might participate to the weak fluorescence of DPA. Knowing the compounds present before UVc treatment, we were able to determine which molecules were produced.

The first effect was the decarboxylation of the acid functions of dipicolinic acid and maybe a double decarboxylation of this compound. As the mass of DPA is around 168 *m/z*, a double decarboxylation would have resulted in a molecular weight around 78 *m/z*, which would have been outside of the mass scan range of 100-1500 *m/z*. Therefore, the double decarboxylation hypothesis could not be verified. These molecules, $C_6H_6NO_2$ and perhaps C_5H_6N (not seen) could have been precursors to other molecules.

The first hypothesis was that the UVc treatment would break the pyridine and favour a polymeric form with an azote at the center of this structure, as shown in the following compounds: $C_8H_{20}N$, $C_{12}H_{28}N$ and $C_{12}H_{28}NO$. The second hypothesis was the production of bipyridine complexes with two isomers in 2,2' or 2,3' for the following compounds: $C_{10}H_9N_2$, $C_{11}H_9N_2O_2$, $C_{11}H_9N_2O_3$, $C_{12}H_9N_2O_4$ and $C_{12}H_9N_2O_5$.

Some molecules, which showed a negligible intensity on the mass spectra, could not be determined based solely on their molecular weights: $C_6H_4NO_2$, $C_7H_4NO_3$ and $C_4H_4N_3O_6$. A literature review of DPA and its photoproducts did not provide any additional information. Other molecules on the MS spectra, whose molecular mass (*m/z*) were 270.5129 and 372.9975, could not be determined. Further experiments, like molecular fragmentation or separation and purification followed by infrared or NMR studies, will be needed to determine these molecules and characterize still undetermined photoproducts.

It should be noted that the irradiation time had an important influence on the production of photoproducts. Even if mass spectrometry direct injection can not be used to accurately quantify the detected compounds, a strong change in intensity gives an indication of the shift in relative proportions. We noticed that the compounds that present the main shift after prolonged irradiation were the picolinic acid and the majority of the bipyridine complexes. There was also an increase in the proportion of the polymeric structure $C_{12}H_{28}NO$. The shift of other compound intensities was not large enough to draw any conclusions. It seems that a longer irradiation time would promote the production of precursors such as picolinic acid and thus increase the proportion of complexes formed from this compound.

Table 1: List of the major compounds found by mass spectrometry by direct injection of DPA solution, before and after UVc treatment at different irradiation times (10 min. and 1h.). ND: Not Determined. NP: Not Proposed, a.u.: arbitrary unit.

					Intensity (a.u.)		
$m/z_{experimental}$ $[M+H]^+$	**Err [ppm]**	**mSigma**	**Ion putative formula**	**Proposed structural formula**	**DPA untreated 1 x 10^{-2} M**	**DPA 10 min UVc**	**DPA 1 h UVc**
122.0236	0.7	5.8	$C_6H_4NO_2$	NP	5.26×10^4	4.58×10^4	7.26×10^4
124.0392	0.8	3.7	$C_6H_6NO_2$	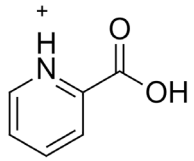	ND	2.51×10^4	2.47×10^5
130.1589	0.7	2.5	$C_8H_{20}N$	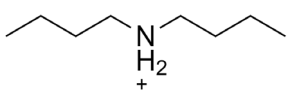	ND	4.67×10^5	1.14×10^5
150.0184	1.2	1.1	$C_7H_4NO_3$	NP	3.10×10^5	2.58×10^5	3.78×10^5
157.0758	1.1	3.6	$C_{10}H_9N_2$	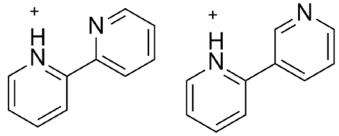	ND	1.25×10^4	3.33×10^5
168.0290	0.6	1.5	$C_7H_6NO_4$	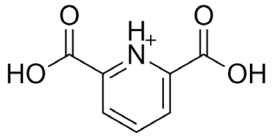	1.36×10^6	1.23×10^6	1.97×10^6
182.0447	0.2	n.a.	$C_8H_8NO_4$	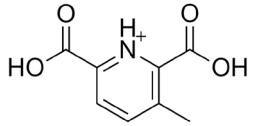	2.28×10^4	ND	3.08×10^5

305 *Table 1 (continue)*

$m/z_{experimental}$ $[M+H]^+$	Err [ppm]	mSigma	Ion putative formula	Proposed structural formula	Intensity (a.u.) DPA untreated 1 x 10^{-2} M	DPA 10 min UVc	DPA 1 h UVc
186.2217	-0.3	0.6	$C_{12}H_{28}N$	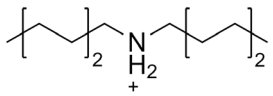	ND	3.88×10^6	2.39×10^6
190.0110	-8.2	12.9	$C_4H_4N_3O_6$	NP	3.87×10^6	1.86×10^6	1.81×10^6
201.0658	0.5	1.7	$C_{11}H_9N_2O_2$	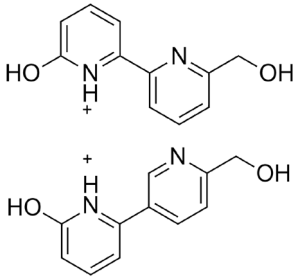	ND	5.28×10^4	4.71×10^5
202.2165	0.3	12.9	$C_{12}H_{28}NO$	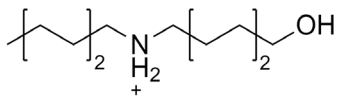	ND	8.83×10^5	4.44×10^4
217.0607	0.4	13.5	$C_{11}H_9N_2O_3$	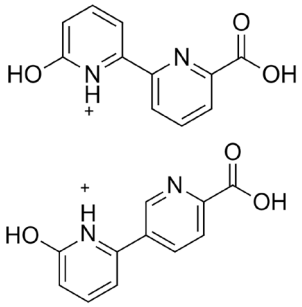	ND	7.71×10^3	7.04×10^4

306

307 *Table 1 (continue)*

					Intensity (a.u.)		
$m/z_{experimental}$ $[M+H]^+$	**Err [ppm]**	**mSigma**	**Ion putative formula**	**Proposed structural formula**	**DPA untreated 1 x 10^{-2} M**	**DPA 10 min UVc**	**DPA 1 h UVc**
245.0556	0.2	13.3	$C_{12}H_9N_2O_4$	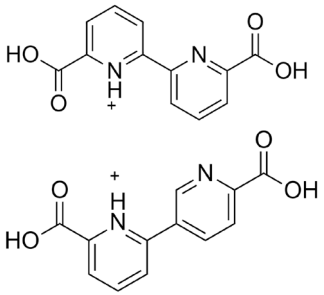	ND	2.37 x 10^4	8.16 x 10^4
261.0505	0.5	15.2	$C_{12}H_9N_2O_5$	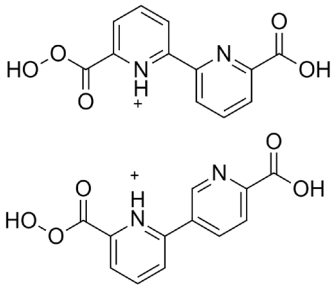	ND	2.30 x 10^4	8.60 x 10^4
270.5129	ND	ND	NP	NP	ND	1.60 x 10^4	5.33 x 10^4
372.9975	ND	ND	NP	NP	ND	1.56 x 10^5	3.19 x 10^5

308

3.4. Application of DPAp and CaDPAp analysis in bacterial spores

UVc treatment made it possible to observe photoproducts formation using fluorescence measurement, as shown in Fig. 5. Nevertheless, the treatment applied *in vitro* (0,120 J/cm² during 10 min) killed all bacterial spores (inactivation of more than 6 log) in our sample as given by CFU experiment (not shown). A DPA assay has been carried out to check if CaDPA and its fluorescent photoproducts were not released outside the spore after this UVc treatment. No release of CaDPA was detected, except for strain PS4150 that shown partial permeability by releasing a very small part of its CaDPA content (data not shown). This CaDPA release after UVc exposure can be explained by a greater impact of UVc on PS4150 spore structure, particularly on the inner membrane, due to the lack of the spore coat. A treatment just as lethal as the previous one was carried out by reducing the irradiation time to 2 minutes, which allows the strain PS4150 to retain its DPA and CaDPA. However, shorter treatments in terms of irradiation time, and especially at non-lethal dose, did not make it possible to clearly distinguish the increase in fluorescence intensity. Thus, although our treatment was lethal, it allowed our bacterial spores to retain the intracellular DPA and CaDPA.

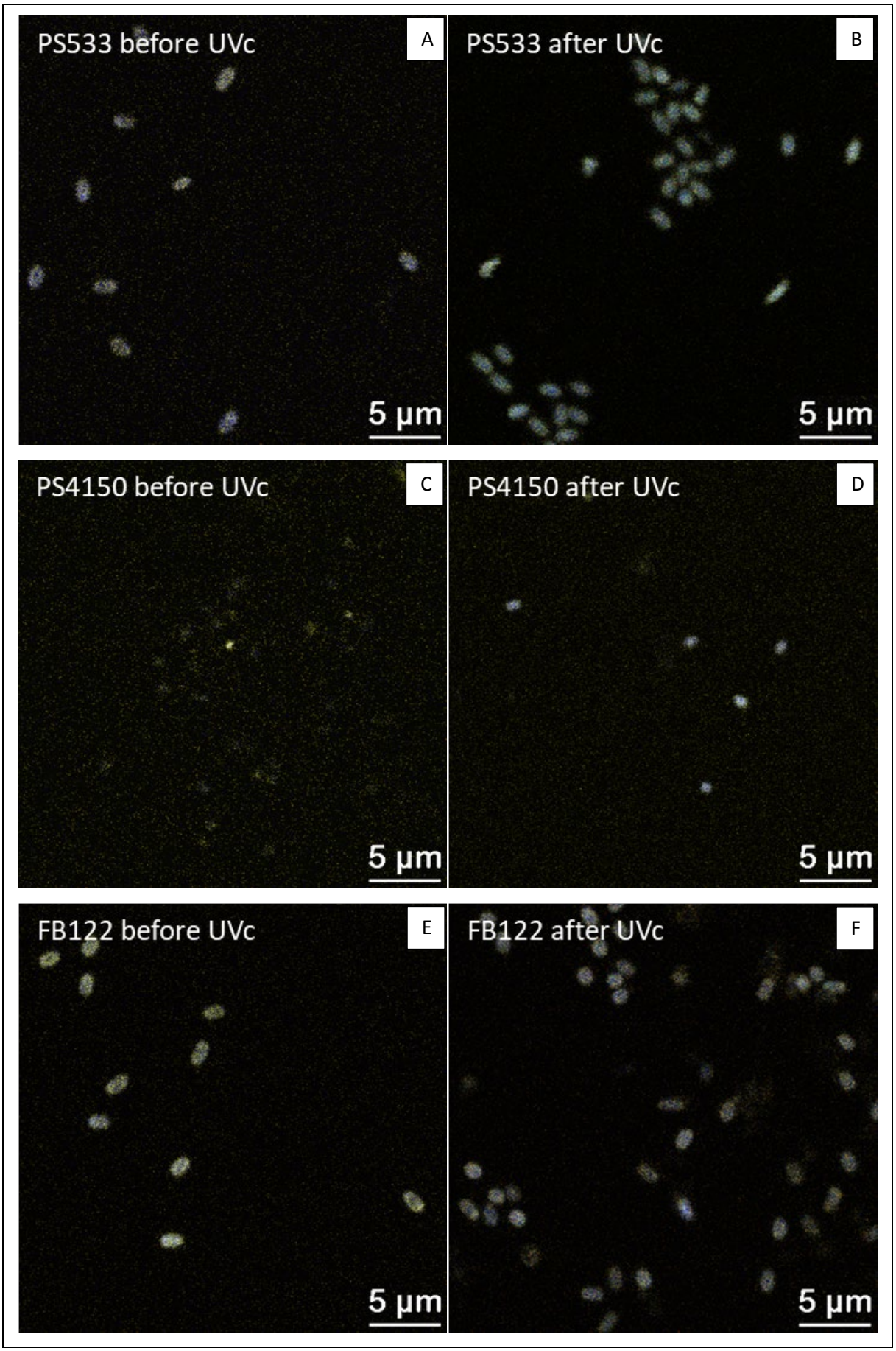
PS533 before UVc
A
5 µm
PS533 after UVc
B
5 µm
PS4150 before UVc
C
5 µm
PS4150 after UVc
D
5 µm
FB122 before UVc
E
5 µm
FB122 after UVc
F
5 µm

Figure 5: Two photon microscopy images for each strain before and after UVc treatment (2 minutes at 0.120 J/cm²) with the same contrast. PS533 (wild-type) before irradiation (A) and after irradiation (B). PS4150 (without coat) before irradiation (C) and after irradiation (D). FB122 (lack of DPA) before irradiation (E) and after irradiation (F).

Fig. 6 showed the fluorescence intensity variations after UVc irradiation of 2 minutes at 0.120 J/cm² for all the strains. It increased in all cases. The reference was the strain PS533 which was a wild type. For this strain, the mean value of fluorescence intensity (a.u.) changes from 532 to 787, as shown in Fig. 6(A). PS4150, the strain whose coat was highly degraded, serves as a control for the spores autofluorescence. In Fig. 6(B), its mean value of fluorescence intensity increased from 117 to 419 (a.u.). Fig. 6(C) clearly showed that our strain control without DPA and CaDPA, FB122, had the weakest increase. Its mean value of fluorescence intensity changed from 568 to 664 (a.u.). Fig. 6(D) showed the increase in fluorescence intensity for each strain before and after UVc treatment. This figure allows us to compare the direct effect of UVc treatment between our different strains and to see the influence of the coat in the resistance to UVc. The PS4150 strain had a much higher increase in fluorescence intensity than the other strains which was approximately 301 ± 55 (a.u.). We have hypothesized that the coat may have absorbed a part of the UVc, which could explain the significant reduction in the production of DPAp and CaDPAp for the strains possessing the coat. The FB122 strain, lacking DPA and CaDPA, had the lowest increase in fluorescence intensity after irradiation, which was around 95 ± 41 (a.u.). This weak UVc effect might be generated by photochemical reactions with the coat or with compounds present in the bacterial spore, or could have been due to the low remaining presence of DPA and CaDPA in this strain [7]. The increase in fluorescence intensity for the PS533 spores which was approximately around 254 ± 53 (a.u.), had suggested that the UVc effect might be mainly governed by the production of DPAp and CaDPAp.

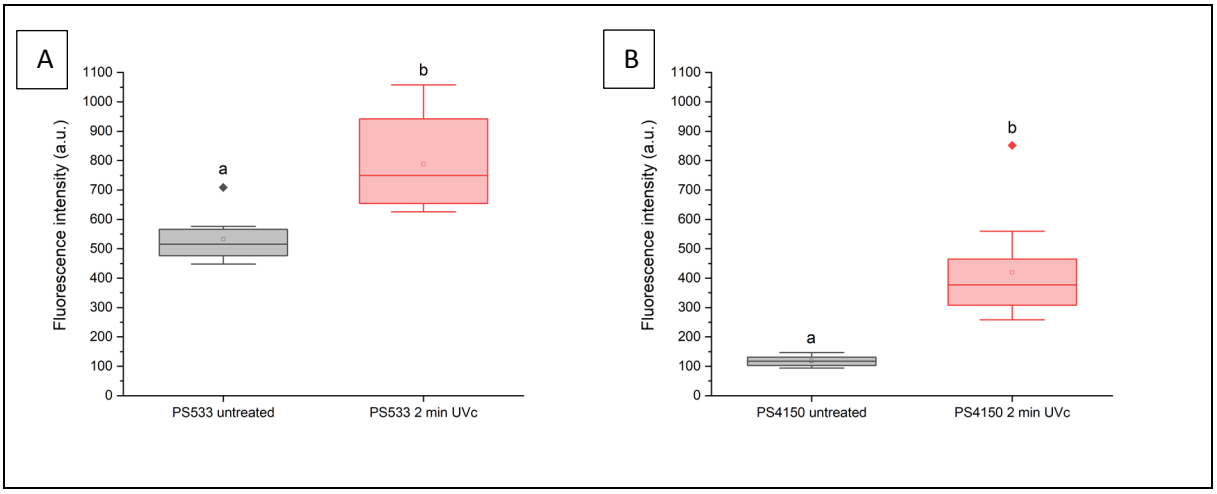

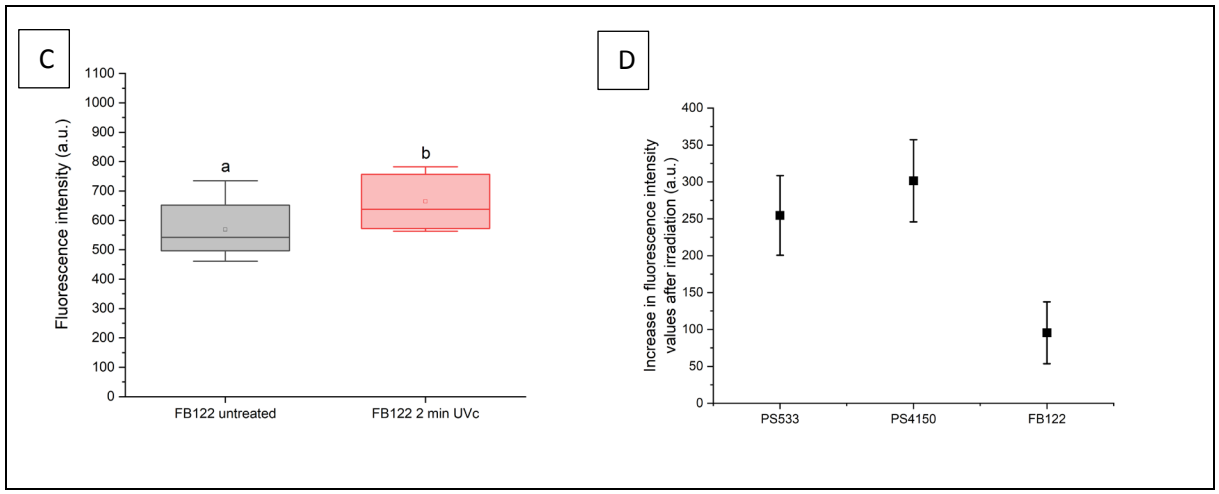

Figure 6: Fluorescence intensity of bacterial spores (N=10) before and after irradiation for strains PS533 (wild-type) (A), PS4150 (without coat) (B), FB122 (lack of DPA) (C). Increase in fluorescence intensity values after irradiation for each strain (D). Different letters above box plot (a,b) represent significant differences (p=0.05) between the time conditions.

Moreover, we have performed an analysis of the contours of each of our phasor plot representations to be able to observe the shifts in our fluorescence lifetimes as a function of irradiation, Fig. 7(A). This allows us to highlight the elongation of lifetimes for strain PS533 that moved mainly on a horizontal axis, suggesting an increase in the proportion of long fluorescence lifetimes. Strain PS4150 seemed to move weakly towards the inside of the semicircle, which means the appearance of multiple fluorescence lifetimes. For strain FB122, the irradiation did not seem to shift the phasor plot representation to higher values, but on the contrary moved it towards a greater proportion of short fluorescent lifetimes. With the lack of DPA, the effect of irradiation could be due to many compounds, such as coat proteins. The associated table, Fig. 7(B), shows the mean fluorescence lifetimes obtained for all the studied strains. For PS533 strain, the mean fluorescence lifetime increased significantly from 1.54 ± 0.15 ns to 1.85 ± 0.19 ns. The two other strains had mean fluorescence lifetime that did not change significantly. The constant PS4150 fluorescence lifetimes before and after irradiation could be explained by a lower production of photoproducts, but this is not consistent with the intensity changes reported (cf. Figure 6). Otherwise, we may assume that natural DPA photoproducts are already present in the bacterial spore, explaining the initial presence of a long lifetime. For PS4150, no short fluorescence lifetime from coat proteins will reduce the spore mean lifetime, as they do for PS533, so irradiation of PS4150 will increase the rate of DPA photoproducts without changing the lifetime. For strain FB122, there was a very small decrease in fluorescence lifetime from 1.48 ± 0.13 ns to 1.43 ± 0.16 ns with a small increase in fluorescence intensity. Thus, we propose that the slight observed changes should be related to proteins rather to residual DPA. These results were in line with our previous observations, since we expected no change for this strain without DPA/CaDPA. The irradiation seemed to increase significantly the fluorescence

intensity and lifetime only for strain PS533, counterbalancing the short lifetime of coat proteins. The PS533 lifetime shifts closer to the PS4150 one, which stay stable after irradiation because of the absence of coat proteins. Conversely, strain FB122 do not change significantly in lifetime nor in intensity due to its deficiency in DPA.

We hypothesize that fluorescence lifetime changes should be driven primarily by the creation of CaDPA photoproducts. To explain this increase, we know that the pH inside the bacterial spore, regardless of its state (dormant or during sporulation), was greater than pH 6 [28,29]. This intracellular pH corresponds to a pH value greater than its pK_{a3} (pK_{a1}: 0.49; pK_{a2}: 2.2 and pK_{a3}: 4.6) [30–32]. In such an environment, the DPA is in a twice deprotonated form (DPA^{2-}) with a mean fluorescence lifetime of 4.3 ns and a mean fluorescence lifetime of 3.2 ns for CaDPA in their irradiated form (data not shown). These lifetimes were greater than those of the spore before irradiation for the strain PS533 and FB122. This allows us to explain the increase in lifetime with to the appearance of photoproducts that will lengthen the lifetimes for strain PS533, and could explain the slight change for the strain PS4150, that had fluorescence lifetimes close to these values.

A

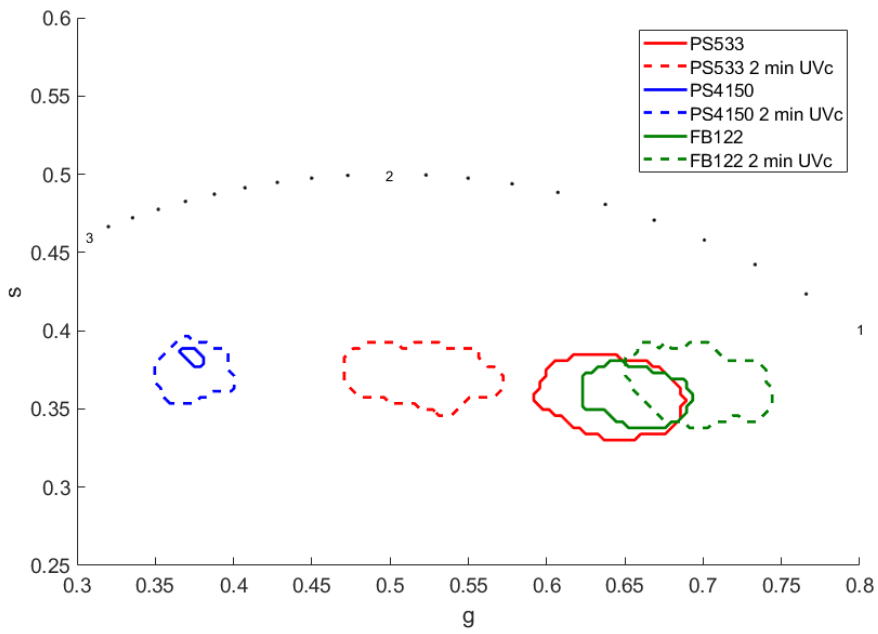

B

	τ_{mean} before irradiation (ns)	τ_{mean} after irradiation (ns)
PS533	1.54 ± 0.15	1.85 ± 0.19
PS4150	2.91 ± 0.24	2.93 ± 0.32
FB122	1.48 ± 0.13	1.43 ± 0.16

Figure 7: (A) Phasor plot image outlines before (line) and after irradiation (dotted line) for each strain: PS533 (red), PS4150 (blue) and FB122 (green). (B) Table: Mean fluorescence lifetime (τ_{mean}) obtained by phasor plot representation for all strains used before and after irradiation (0.120 J/cm² for 2 min). Where g and s represent the values at the two coordinates [g;s] of the phasor plot.

4. Conclusions

In conclusion, this study demonstrates the instability of the photoproducts of DPA and CaDPA, which continue to reorganize as DPAp and CaDPAp, 24 hours after irradiation. To complete this observation, we measured the consumption of DPA for the production of these compounds, in amounts linked to the irradiation time. The loss of DPA was about 60% of the initial concentration after 10 minutes of irradiation. This study also demonstrates the rearrangement of unstable photoproducts into the form of DPA 24 hours after irradiation. It allows us to hypothesize that the DPA excited via UVc produces photoproducts, but that part of this DPA* will take longer to either rearrange in the form of DPAp or in the form of DPA. Mass spectrometry experiments confirm the presence of photoproducts already identified and suggest the presence of still unidentified molecules. All of these data enable us to better understand the effects of UVc on DPA and its CaDPA salt, which may be useful for further studies on bacterial spores. This work also highlights the benefits of using fluorescence microscopy and fluorescence lifetime imaging to study the inner compartment of bacterial spores and more specifically to use the DPA photoproducts as environmental probes.

Acknowledgement

The authors wish to thank the DIVVA platform (Développement Innovation Vigne Vin Aliments) for the mass spectrometry analyses and especially Dr. Remy Romanet for the technical support as well as the critical reading of the manuscript. We also thank Dr. Ambroise Marin for his help on the development of the phasor plot image analysis tool. The authors are very grateful to Maud Pegeot for the careful proofreading and correction of the manuscript. The authors also acknowledge the region “Bourgogne Franche-Comté” and the University of Burgundy for its funding.

References

[1] W.L. Nicholson, N. Munakata, G. Horneck, H.J. Melosh, P. Setlow, Resistance of *Bacillus* Endospores to Extreme Terrestrial and Extraterrestrial Environments, Microbiol Mol Biol Rev. 64 (2000) 548–572. https://doi.org/10.1128/MMBR.64.3.548-572.2000.

[2] P. Setlow, Spores of Bacillus subtilis: their resistance to and killing by radiation, heat and chemicals, J Appl Microbiol. 101 (2006) 514–525. https://doi.org/10.1111/j.1365-2672.2005.02736.x.

[3] L. Kong, P. Setlow, Y. Li, Analysis of the Raman spectra of Ca2+-dipicolinic acid alone and in the bacterial spore core in both aqueous and dehydrated environments, Analyst. 137 (2012) 3683. https://doi.org/10.1039/c2an35468c.

[4] P. Setlow, Spore Resistance Properties, Microbiol Spectr. 2 (2014). https://doi.org/10.1128/microbiolspec.TBS-0003-2012.

[5] J.H. Tiburski, A. Rosenthal, S. Guyot, J.-M. Perrier-Cornet, P. Gervais, Water Distribution in Bacterial Spores: A Key Factor in Heat Resistance, Food Biophysics. 9 (2014) 10–19. https://doi.org/10.1007/s11483-013-9312-5.
[6] P. Zhang, L. Kong, P. Setlow, Y. Li, Characterization of Wet-Heat Inactivation of Single Spores of Bacillus Species by Dual-Trap Raman Spectroscopy and Elastic Light Scattering, Appl Environ Microbiol. 76 (2010) 1796–1805. https://doi.org/10.1128/AEM.02851-09.
[7] M. Paidhungat, B. Setlow, A. Driks, P. Setlow, Characterization of Spores of Bacillus subtilis Which Lack Dipicolinic Acid, J Bacteriol. 182 (2000) 5505–5512. https://doi.org/10.1128/JB.182.19.5505-5512.2000.
[8] B. Setlow, S. Atluri, R. Kitchel, K. Koziol-Dube, P. Setlow, Role of Dipicolinic Acid in Resistance and Stability of Spores of Bacillus subtilis with or without DNA-Protective α/β-Type Small Acid-Soluble Proteins, J Bacteriol. 188 (2006) 3740–3747. https://doi.org/10.1128/JB.00212-06.
[9] T.A. Slieman, W.L. Nicholson, Role of Dipicolinic Acid in Survival of *Bacillus subtilis* Spores Exposed to Artificial and Solar UV Radiation, Appl Environ Microbiol. 67 (2001) 1274–1279. https://doi.org/10.1128/AEM.67.3.1274-1279.2001.
[10] S. Huang, D. Chen, P.L. Pelczar, V.R. Vepachedu, P. Setlow, Y. Li, Levels of Ca2+-Dipicolinic Acid in Individual Bacillus Spores Determined Using Microfluidic Raman Tweezers, JB. 189 (2007) 4681–4687. https://doi.org/10.1128/JB.00282-07.
[11] C.B. Smith, J.E. Anderson, J.D. Edwards, K.C. Kam, In Situ Surface-Etched Bacterial Spore Detection Using Dipicolinic Acid–Europium–Silica Nanoparticle Bioreporters, Appl Spectrosc. 65 (2011) 866–875. https://doi.org/10.1366/10-06167.
[12] M.L. Cable, J.P. Kirby, K. Sorasaenee, H.B. Gray, A. Ponce, Bacterial Spore Detection by [Tb $^{3+}$ (macrocycle)(dipicolinate)] Luminescence, J. Am. Chem. Soc. 129 (2007) 1474–1475. https://doi.org/10.1021/ja061831t.
[13] T.A. Alexander, P.M. Pellegrino, J.B. Gillespie, Near-Infrared Surface-Enhanced-Raman-Scattering-Mediated Detection of Single Optically Trapped Bacterial Spores, Appl Spectrosc. 57 (2003) 1340–1345. https://doi.org/10.1366/000370203322554482.
[14] R. Goodacre, B. Shann, R.J. Gilbert, É.M. Timmins, A.C. McGovern, B.K. Alsberg, D.B. Kell, N.A. Logan, Detection of the Dipicolinic Acid Biomarker in *Bacillus* Spores Using Curie-Point Pyrolysis Mass Spectrometry and Fourier Transform Infrared Spectroscopy, Anal. Chem. 72 (2000) 119–127. https://doi.org/10.1021/ac990661i.
[15] M.W. Tabor, J. MacGee, J.W. Holland, Rapid determination of dipicolinic acid in the spores of Clostridium species by gas-liquid chromatography., Appl Environ Microbiol. 31 (1976) 25–28. https://doi.org/10.1128/aem.31.1.25-28.1976.
[16] H. Paulus, Determination of dipicolinic acid by high-pressure liquid chromatography, Analytical Biochemistry. 114 (1981) 407–410. https://doi.org/10.1016/0003-2697(81)90502-9.
[17] R. Nudelman, B.V. Bronk, S. Efrima, Fluorescence Emission Derived from Dipicolinic Acid, its Sodium, and its Calcium Salts, Appl Spectrosc. 54 (2000) 445–449. https://doi.org/10.1366/0003702001949564.
[18] S. Sarasanandarajah, J. Kunnil, B.V. Bronk, L. Reinisch, Two-dimensional multiwavelength fluorescence spectra of dipicolinic acid and calcium dipicolinate, Appl. Opt. 44 (2005) 1182. https://doi.org/10.1364/AO.44.001182.
[19] A. Alimova, A. Katz, H.E. Savage, M. Shah, G. Minko, D.V. Will, R.B. Rosen, S.A. McCormick, R.R. Alfano, Native fluorescence and excitation spectroscopic changes in Bacillus subtilis and Staphylococcus aureus bacteria subjected to conditions of starvation, Appl. Opt. 42 (2003) 4080. https://doi.org/10.1364/AO.42.004080.
[20] G.R. Germaine, W.G. Murrell, Use of Ultraviolet Radiation to Locate Dipicolinic Acid in Bacillus cereus Spores, J Bacteriol. 118 (1974) 202–208. https://doi.org/10.1128/jb.118.1.202-208.1974.
[21] G. Nardi, M. Lineros-Rosa, F. Palumbo, M.A. Miranda, V. Lhiaubet-Vallet, Spectroscopic characterization of dipicolinic acid and its photoproducts as thymine photosensitizers, Spectrochimica Acta Part A: Molecular and Biomolecular Spectroscopy. 245 (2021) 118898. https://doi.org/10.1016/j.saa.2020.118898.

[22] A.C. Noell, T. Ely, D.K. Bolser, H. Darrach, R. Hodyss, P.V. Johnson, J.D. Hein, A. Ponce, Spectroscopy and Viability of *Bacillus subtilis* Spores after Ultraviolet Irradiation: Implications for the Detection of Potential Bacterial Life on Europa, Astrobiology. 15 (2015) 20–31. https://doi.org/10.1089/ast.2014.1169.
[23] S. Ghosh, B. Setlow, P.G. Wahome, A.E. Cowan, M. Plomp, A.J. Malkin, P. Setlow, Characterization of Spores of *Bacillus subtilis* That Lack Most Coat Layers, J Bacteriol. 190 (2008) 6741–6748. https://doi.org/10.1128/JB.00896-08.
[24] J.S. Reidmiller, J.D. Baldeck, G.C. Rutherford, R.E. Marquis, Characterization of UV-Peroxide Killing of Bacterial Spores, Journal of Food Protection. 66 (2003) 1233–1240. https://doi.org/10.4315/0362-028X-66.7.1233.
[25] A.A. Hindle, E.A.H. Hall, Dipicolinic acid (DPA) assay revisited and appraised for spore detection, Analyst. 124 (1999) 1599–1604. https://doi.org/10.1039/a906846e.
[26] A. Leray, S. Padilla-Parra, J. Roul, L. Héliot, M. Tramier, 827Spatio-Temporal Quantification of FRET in Living Cells by Fast Time-Domain FLIM: A Comparative Study of Non-Fitting Methods, PLoS ONE. 8 (2013) e69335. https://doi.org/10.1371/journal.pone.0069335.
[27] H.F. Hameka, J.O. Jensen, J.L. Jensen, C.N. Merrow, C.P. Vlahacos, Theoretical studies of the fluorescence of dipicolinic acid and its anion, Journal of Molecular Structure: THEOCHEM. 365 (1996) 131–141. https://doi.org/10.1016/0166-1280(96)04487-9.
[28] N.G. Magill, A.E. Cowan, D.E. Koppel, P. Setlow, The internal pH of the forespore compartment of Bacillus megaterium decreases by about 1 pH unit during sporulation., J Bacteriol. 176 (1994) 2252–2258. https://doi.org/10.1128/jb.176.8.2252-2258.1994.
[29] B. Setlow, P. Setlow, Measurements of the pH within dormant and germinated bacterial spores., Proc Natl Acad Sci U S A. 77 (1980) 2474–2476. https://doi.org/10.1073/pnas.77.5.2474.
[30] Shigenobu. Funahashi, Kensaku. Haraguchi, Motoharu. Tanaka, Reactions of hydrogen peroxide with metal complexes. 2. Kinetic studies on the peroxo complex formation of nitrilotriacetatodioxovanadate(V) and dioxo(2,6-pyridinedicarboxylato)vanadate(V), Inorg. Chem. 16 (1977) 1349–1353. https://doi.org/10.1021/ic50172a019.
[31] K.S. Rajan, R. Jaw, N. Grecz, Role of Chelation and Water Binding of Calcium in Dormancy and Heat Resistance of Bacterial Endospores, Bioinorganic Chemistry. 8 (1978) 477–491. https://doi.org/10.1016/0006-3061(78)80002-7.
[32] T. Tang, K.S. Rajan, N. Grecz, Mixed Chelates of Ca(II)-Pyridine-2,6-Dicarboxylate with Some Amino Acids Related to Bacterial Spores, Biophysical Journal. 8 (1968) 1458–1474. https://doi.org/10.1016/S0006-3495(68)86566-X.

UVc 254 nm

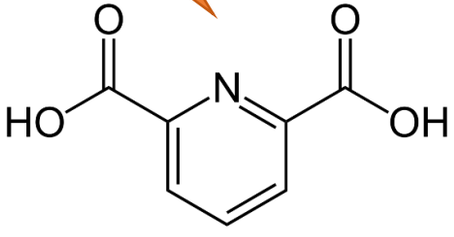

2,6-pyridinedicarboxylic acid **(DPA)**

UVc effects

DPA photoproducts **(DPAp)**

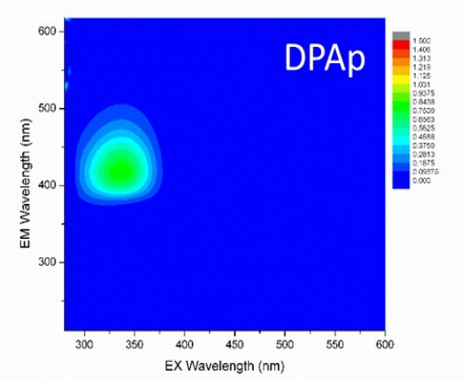

DPAp instability

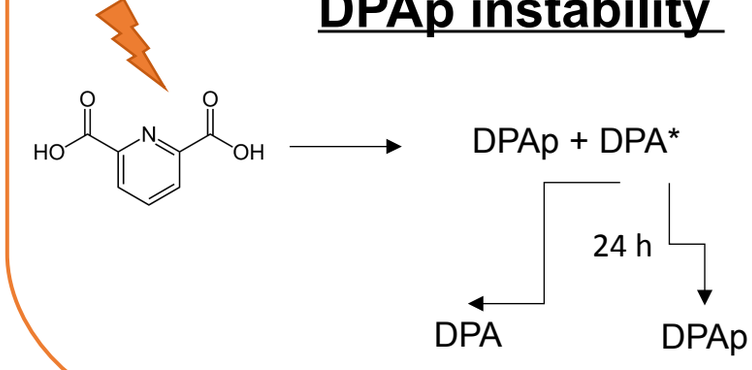

DPAp visualization

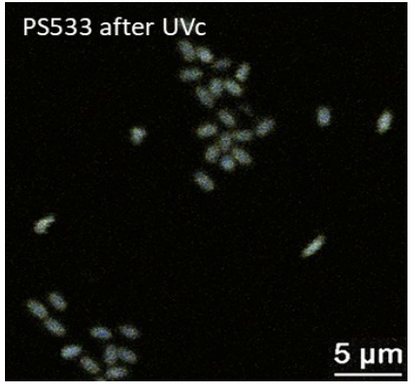

Multi-photon microscopy on bacterial spores

FLIM & Phasor plot on bacterial spores